Electronic Supplementary Material (ESI) for Nanoscale.

Supplementary information

Fast Water Channeling across Carbon Nanotubes in Far Infrared Terahertz Electric Fields

Qi-Lin Zhang, Rong-Yao Yang, Wei-Zhou Jiang*, Zi-Qian Huang

1. More simulations with various TEF setups

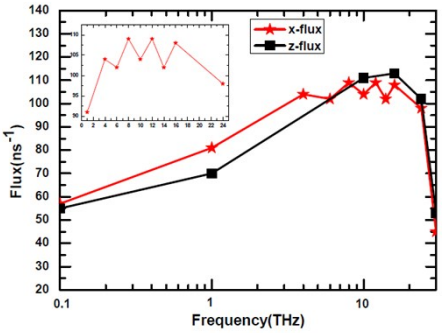

Fig. S1 The net flux as a function of the EF frequency, where the EF is uniformly applied to the whole system space. The curves with stars and squares stand for results with the EF along x- and z-axes, respectively.

In our simulations, only the space between two reservoirs is exposed to the spatially uniform TEF. It is not easy to constrain the TEF to the region of a short nanotube in experiments. Fortunately, we find that the dramatic flux enhancement, subject to the resonant mechanisms, still holds for much longer SWCNT (e.g. with the length of 10 *nm*). Thus, the situation for experiments can be improved by focusing high power terahertz rays to the space divided by much longer SWCNT.

In fact, more simulations have been performed by extending the TEF into the water reservoir. Shown in the Fig. S1 is the net flux with the TEF being extended to the whole reservoir. We see that the net fluxes are dramatically enhanced in the frequency range from about 0.1 *THz* to 30 *THz*, and the peak values with a wiggling flattop, appearing in the frequency interval of 4-24 *THz*, are about 105 ns^{-1}, being approximately five times the zero-field result. In this case, it is observed that the water transport is almost independent of the TEF orientation. These results are very different from those with the TEF only shining to the space between two reservoirs. The occurrence of this extraordinary phenomenon is due to the rupture of hydrogen bonds that makes individual water molecules in the reservoir to break into the nanotube. This provides an evidence of the efficient energy acquisition through the resonant mechanism. However, the resulting temperature of reservoir water rises dramatically for the sufficient energy acquisition at resonant frequencies, and the Langevin thermostat is not able to maintain the constant temperature.

Alternatively, we have also conducted a series of simulations with the TEF extending into the reservoir water by a few angstroms. As an example, Fig. S2 shows the net flux with the TEF extending into the reservoir by 2*Å*. Here, the flux evolution with the frequency is consistent with that with the TEF setup we adopted in the manuscript (see Fig. 2). This indicates that with a limited extension of TEF into the reservoir, the water transport is not much affected.

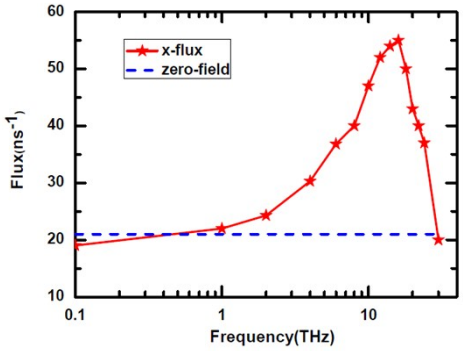

Fig.S2 The net flux as a function of the EF frequency, where the EF along x-axis is extended into the reservoir by 2 *Å*. The dash line denotes the zero-field result.

Based on these researches, we adopt the present setup that the TEF only shines to the space between two reservoirs. This setup can be used to highlight the resonant mechanisms that are important for water transport, while it evades the unnecessary thermal effect, since only a few water molecules in the SWCNT, rather than reservoir water, acquire the energy.

2. Energy transfer from the TEF

Since the rupture of hydrogen bonds is a result of the energy transfer from the TEF, it is significant to evaluate quantitatively the work done by the TEF, which is the relative energy of water molecules above the zero-field one. We have calculated the average total energy per water molecule at some specific frequencies, as shown in Fig. S3. In the simulation, the water molecules are held inside the nanotube. We can see from Fig. S3 that the energy transfer is prominent in the frequency region of resonance. The curve is peaked around 14 THz, in accord with the frequency profile of the flux in Fig.2. This result provides a quantitative evidence that the energy transfer from the TEF plays a major role in the enhanced water flow.

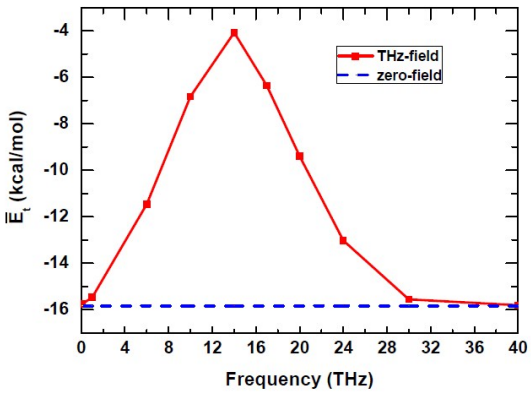

Fig.S3 The average total energy per water molecule inside the nanotube as a function of the EF frequency. The dash line denotes the zero-field result.

3. Water model dependence of the results

In order to examine the model dependence of our main results, we perform some comparative simulations using the SPC/E water model. The results at some representative frequencies are tabulated in TABLE S1. As

the Tip3p model gives faster diffusion [S1], we can see that the magnitude of the flux is larger than the one with the SPC/E model. However, the tendencies of the net flux and the hydrogen-bond (HB) and occupation numbers with both models are consistent with each other. Thus, the main conclusions that we have drawn in the manuscript do not depend on the specific water model.

TABLE S1: The simulation results of Tip3p and SPC/E water models.

	Flux (Tip3p)	Flux (SPC/E)	HB number (Tip3p)	HB number (SPC/E)	Occupancy (Tip3p)	Occupancy (SPC/E)
Zero-field	21	6	3.0	2.87	4.97	4.34
8 THz	35	16	1.44	1.03	4.41	3.24
10 THz	49	19	0.82	0.52	3.76	2.43
14 THz	57	20	0.40	0.38	3.5	2.22
20 THz	44	18	1.26	1.08	4.4	3.61
30 THz	23	7	2.97	2.90	4.94	4.43

4. Relationship between the flux and field strength at resonant frequencies

In order to check the dependence of water transport properties on the TEF amplitude, we have performed simulations with various TEF amplitudes at 14 *THz* which is the centroid of resonant frequencies. Fig. S4 displays the net flux, the average occupation number $\bar{N}$ and hydrogen bond number $\bar{N}_H$of water molecules inside the SWCNT as a function of the TEF amplitude. Though the relationship between these quantities and the TEF amplitude is not linear, they evolve almost linearly at moderate TEF amplitudes. They are close to the zero-field values when the TEF amplitude $E_0 < 0.1$ *V/nm*.

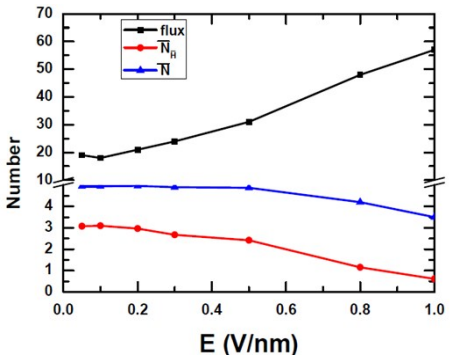

Fig. S4The net flux, average occupancy number $\bar{N}$ and hydrogen bond number $\bar{N}_H$ of water molecules inside the SWCNT as a function of the electric field amplitude at 14 *THz*. The electric field is along x-axis.

5. **Net fluxes under various pressure gradients at resonant frequencies**

Under the equilibrium condition, the in-tube water transports in correlated bursts of the hydrogen-bonded filament, the net flux increases linearly with the pressure gradient, which can be demonstrated by the

collective diffusion model proposed by *Zhu et al.*[9]. In the method in Ref. [9], the diffusion coefficient is calculated under the equilibrium condition. At non-resonant frequencies, the net fluxes with different pressure gradients in our simulations are consistent with those obtained from the method proposed by Ref. [9]. At resonant frequencies, the efficient energy transfer from the TEF spoils the spontaneous diffusion due to the thermal fluctuation at equilibrium, and we cannot follow the collective diffusion model to perform calculations under the non-equilibrium condition.

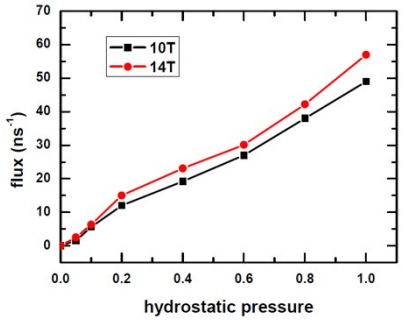

Fig.S5 The net flux as a function of hydrostatic pressure at the frequency 10 and 14 *THz* and field strength 1 *V/nm*, where the pressures labelled in the horizontal axis are in unit of the applied pressure in the paper.

The dramatic rise of the net flux at resonant frequencies occurs with the rupture of hydrogen bonds due to the energy transfer from the TEF. In this case, we find that the relation between the net flux and pressure gradient is not far off linear in a large domain of pressure gradients, as shown in Fig. S5, though the equilibrium diffusion now does not apply at null pressure.Fig.S5 displays the net flux as a function of hydrostatic pressure at resonant frequencies 10 *THz* and 14 *THz*. Compared to net fluxes at non-resonant frequencies, the significant flux enhancement remains at lower pressure gradients.

References

S1. P. Mark and L. Nilsson, J. Phys. Chem. A 2001, 105, 9954-9960.